Probing Adsorption of Methane onto Vanadium Cluster Cations via Vibrational Spectroscopy

Justine Kozubal, Tristan Heck, and Ricardo B. Metz*[a)]

University of Massachusetts Amherst Department of Chemistry, Amherst, Massachusetts 01003, United States

Photofragment spectroscopy is used to measure the vibrational spectra of $V_2^+(CH_4)_n$ (n=1-4), $V_3^+(CH_4)_n$ (n=1-3), and $V_x^+(CH_4)$ (x=4-8) in the C−H stretching region (2550-3100 cm^{-1}). Spectra are measured by monitoring loss of CH_4. The experimental spectra are compared to simulations at the B3LYP+D3/6-311++G(3df,3pd) level of theory to identify the geometry of the ions. MRCI+Q calculations are also carried out on V_2^+ and V_3^+. The methane binding orientation in $V_2^+(CH_4)_n$ (n=1-4) evolves from η^3 to η^2 as more methane molecules are added. The IR spectra of metal-methane clusters can give information on the structure of metal clusters that may otherwise be hard to obtain from isolated clusters. For example, the $V_3^+(CH_4)_n$ (n=1-3) experimental spectra show an additional peak as the second and third methane molecules are added to V_3^+, which indicates that the metal atoms are not equivalent. The $V_x^+(CH_4)$ show a larger red shift in the symmetric C−H stretch for larger clusters with x=5-8 than for the small clusters with x=2, 3, indicating increased covalency in the interaction of larger vanadium clusters with methane.

Keywords: vibrational spectroscopy, methane, vanadium, clusters, MRCI, DFT, C-H activation

[a)]Electronic mail: rbmetz@chem.umass.edu

I. INTRODUCTION

Conversion of methane to more useful compounds is both commercially important and technologically difficult, due to its high C-H bond strength. Indirect processes are highly energy intensive,[1,2] so the direct, efficient and selective conversion of methane to a liquid fuel is a long-time and as yet unrealized goal of catalysis.[1,3]

Gas-phase studies have observed that several of the *5d* transition metal cations (Ta^+, W^+, Os^+, Ir^+ and Pt^+) activate C-H bonds in methane at room temperature, producing MCH_2^+ and H_2.[4–7] The reaction is endothermic for the *3d* and *4d* transition metals. However, metal clusters display a wider range of mechanisms for C-H bond activation than atoms, due to cooperative effects and the ability of hydrocarbon fragments to form bonds to different metal atoms. As a result, in several instances, metal clusters are more reactive than the corresponding atom. For example, Pd_2^+ and Pd_3^+ react with methane, while Pd^+ and Pd_4^+ do not.[8] Additionally, reactivity that depends strongly on cluster size, as is observed with Pt_x^+, has been proposed as a sign of a good heterogeneous catalyst.[9,10]

Gas-phase studies of metal cluster ions offer many advantages. Clusters with well-defined composition can be readily produced and their reactions, structure and optical properties investigated.[11] They also permit the stabilization and study of reaction intermediates and facilitate close connection between experiment and theory. Gas-phase studies have uncovered novel reaction mechanisms such as two-state reactivity[12] and have illuminated reaction pathways that are also important in the condensed phase.[13–16]

There have been several studies of reactions of metal cluster ions with methane, and they have been the subject of extensive reviews.[15–20] Armentrout and coworkers studied reactions of Fe_x^+ (x=2-15)[21] and Ni_x^+ (x=2-16)[22] with CD_4 as a function of collision energy by guided ion beam tandem mass spectrometry (GIBMS). Although all of the reactions are endothermic, Fe_x^+ with x=3-5 are found to be especially reactive. These studies also provide covalent bond strengths of the metal clusters to C, CD, CD_2 and CD_3. They reach asymptotic values with increasing cluster size, providing a estimate of the chemisorption energies to metal surfaces. The remaining experiments have been kinetics studies, typically at room temperature, with dehydrogenation the primary product channel. In their study of Co_x^+ (x=2-22), Nakajima *et al.*[23] observed enhanced reactivity for x=4, 5, and $\geq$7. As noted above, Lang *et al.*[8] observed that Pd_2^+ and Pd_3^+ react, while Pd_4^+ does not. Similarly, Rh_2^+

reacts with methane at room temperature, as do $Rh_2Ar_n^+$ and $Rh_3Ar_n^+$, while Rh^+ does not.[24,25] For Ta_x^+ (x=1-10), Eckhard *et al.*[26] found that small clusters (x=1-4) dehydrogenate methane and that reactivity decreases from Ta^+ to Ta_4^+. Larger clusters (x≥4) only adsorb CH_4. Achatz *et al.*[27] and Kummerlowe *et al.*[9] observe that Pt_x^+ (x=1-24) are generally very reactive, with most reacting near the collision rate, although x=4, 10, 13, 14 are significantly less reactive.

Vanadium cluster ions have been studied by several groups. Although their reactions with methane have not been examined, V_x^+ shows size-selective reactivity with D_2. Zakin *et al.* measured reactions of V_x^+ with D_2 at thermal energies and observed no reactions for x<4; for larger clusters, odd clusters are an order of magnitude more reactive than the even ones.[28] Liyanage *et al.*[29] studied the reactions of V_x^+ (x=2-13) with D_2 by GIBMS. They also found odd clusters to be more reactive than even clusters and that reactivity increased with cluster size. Su *et al.*[30] measured metal-metal bond dissociation energies (BDE) by GIBMS. They found that the BDE(V_2^+-V) is anomalously low. Additionally, even clusters are generally more stable than odd clusters and the high stability of the V_x^+ (x=4, 6, 13 and 15) clusters suggest highly symmetrical structures. Additional photoionization studies will be discussed below.

Vibrational spectra of V_x^+ (x=3 to 23) from 140 to 450 cm^{-1} were measured by Fielicke and co-workers using infrared multiple-photon dissociation (IRMPD)[31] and argon tagging[32] using the Free Electron Laser for Infrared Experiments (FELIX). The structures are determined by comparing the measured spectra with calculated results using DFT. The calculations[32] found that slightly distorted structures are favored over highly symmetrical ones, the lowest possible multiplicity is preferred, and the V_x^+ (x=8, 10, and 13) clusters are especially stable. Chaves *et al.*[33] carried out an extensive DFT study of all 30 neutral transition metal clusters (M_x, x=2-15). V_2 was found to have the highest binding energy of the dimers and to have a very short bond length due to strong *d-d* interactions. For clusters up to V_6, the global minimum configurations follow a growth based motif based on dimers. Other calculations will be discussed below.

It is very challenging to determine the geometry and spin state of metal clusters using IR spectroscopy. The vibrations are at low wavenumber, generally have low intensity, and different spin states often have similar calculated spectra. An attractive, albeit indirect, alternative is to produce clusters with physisorbed chromophores and use the vibrations of

the chromophore (typically CO, H_2 or N_2) to report on the structure of the underlying metal cluster.[34–36] As will be shown below, methane can also fulfill this role.

There have been several spectroscopic studies of $M_x^+(CH_4)$ complexes that seek to determine the extent of C-H activation and the structure of the underlying metal cluster, and they are included in two recent reviews.[7,11] Vibrational spectroscopy of the C-H stretches in $Fe_x^+(CH_4)_n$ (x=2-4) found that the red shift increases with increasing cluster size.[37–39] The larger red shift correlates with higher reactivity observed by GIBMS.[21] The remaining studies are in the fingerprint region, and are measured using free-electron lasers, with dissociation often occurring due to IRMPD. Lushchikova *et al.*[40] studied the interaction of Cu_x^+ clusters (x=2-4) with CH_4. For all cluster sizes, they found the methane adsorbs intact in an η^2 configuration and has small deformations which red shift the HCH bending frequencies only slightly from those in bare methane. Harding *et al.*[41] measured the spectra of Pt_x^+ (x=3-5) clusters with CH_4. They found the methane is intact and binds in an η^2 orientation, although a dissociatively adsorbed isomer is calculated to be lower in energy for Pt_3^+.

Only a few vibrational spectra of ligated vanadium cation clusters have been measured. Swart *et al.*[42] measured spectra of saturated, chemisorbed $V_xH_n^+$ and also determined that CO chemisorbs onto most bare V_x^+ clusters and physisorbs on clusters saturated with hydrogen. Jaeger *et al.*[43] obtained spectra of V_x^+ (x=3-18) clusters with one to three H_2O attached. Their measurements of the HOH bend indicate that the water molecules are adsorbed intact.

In this study, we report vibrational spectra of $V_2^+(CH_4)_n$ (n=1-4), $V_3^+(CH_4)_n$ (n=1-3), and $V_x^+(CH_4)$ (x=4-8), measured via photofragment spectroscopy in the C−H stretching region (2550-3100 cm^{-1}). The experimental results are compared to simulated spectra of multiple isomers in various spin states to determine the lowest energy structure.

II. EXPERIMENTAL AND COMPUTATIONAL METHODS

The ions of interest are produced in a laser ablation source and their vibrational photodissociation spectra are measured on a home-built dual time-of-flight reflectron mass spectrometer[44] coupled to an IR laser system. The experimental conditions are briefly described below. Details are in the SI (Section S1).

The molecules are formed by laser ablating a vanadium rod to form cations which then

undergo collisions with backing gas (CH_4, He) introduced through a pulsed valve. Ions travel through a tube to enhance clustering, then expand into vacuum and are extracted into the time-of-flight mass spectrometer. The mass selected ions are dissociated at the turning point of the reflectron by a Nd:YAG OPO/OPA IR laser system (LaserVision). The parent and fragment ions are re-accelerated to hit a dual microchannel plate detector. The fragment signal is normalized to the parent signal and laser power as a function of wavelength to obtain the photodissociation spectrum.

Calculations are carried out with the *Gaussian09* program package.[45] Optimized geometries of the ions are computed using the B3LYP[46] density functional including dispersion (GD3)[47] and the 6-311++G(3df,3pd) basis set. Vibrational frequencies are scaled by 0.965 based on the ratio of the experimental and computed values of the symmetric and antisymmetric C−H stretching frequencies of CH_4. All reported energies include zero-point energy. In addition, all structures and spectra were calculated using the BPW91 functional with dispersion (GD2)[48–50] and the 6-311++G(3df,3pd) basis set, with scaling factor 0.983; the results are included in the SI. We also carried out MRCI+Q (multi-reference configuration interaction with Davidson correction) calculations on $V_2^{0,+}$ and $V_3^{0,+}$ using the MOLPRO electronic structure package.[51,52] The MRCI+Q calculations are described in detail in the SI (Section S2).

III. RESULTS AND DISCUSSION

Photofragment spectroscopy is used to measure the spectra of $V_2^+(CH_4)_{1\text{-}4}$, $V_3^+(CH_4)_{1\text{-}3}$, $V_4^+(CH_4)_{1\text{-}2}$ and $V_{5\text{-}8}^+(CH_4)$ in the C−H stretching region. The results for $V_x^+(CH_4)$ are shown in Figure 1. The C−H stretches of isolated methane are at 2917 cm^{-1} (symmetric stretch) and 3019 cm^{-1} (triply degenerate antisymmetric stretch). Interaction with the metal lowers the symmetry of the CH_4, typically leading to four distinct C−H stretches, makes all of the vibrations IR active (although some have low intensity) and leads to a substantial red shift in the lowest-frequency C−H stretch. This shift is $\geq$100 cm^{-1} and depends non-monotonically on the cluster size, as shown by comparing the peaks to the vertical line at 2800 cm^{-1} in the figure. The spectrum of $V^+(CH_4)(Ar)$ measured previously by our group[53] is the most red shifted while $V_2^+(CH_4)$ and $V_3^+(CH_4)$ have sharp peaks and the smallest red shifts. The spectrum of $V_4^+(CH_4)$ is very broad and possibly consists

of two overlapping peaks. The red shift then increases for $V_5^+(CH_4)$ to $V_8^+(CH_4)$. This increased red shift for n≥3 suggests increased covalency in the interaction between the metal and methane. This is also observed for Fe_x^+ (x=2-4), for which increased red shift correlates with increased reactivity.[37–39] $V^+(CH_4)(Ar)$ has a small peak near 3000 cm^{-1}; its intensity decreases in $V_2^+(CH_4)$, and it is not observed in the larger clusters.

The two limiting cases for methane binding to an atomic cation are with two (η^2, C_{2v} symmetry) or three (η^3, C_{3v} symmetry) hydrogens coordinated to the metal. The coordination can also be between these two limiting cases, so it is useful to specify the angle between the metal, carbon, and the hydrogen farthest from the metal, ∠M−C−H, which is ∼124° for η^2 and 180° for η^3 coordination. These binding motifs are reflected in the spectra where, generally, an η^2 methane complex will have a doublet at ≤2800 cm^{-1} and an η^3 methane complex will have peaks near 2800 and 3000 cm^{-1}. The spectra, structures, and corresponding simulations of the complexes will be discussed in the following sections.

A. $V^+(CH_4)_n$ (n=1-4)

A complete analysis of the $V^+(CH_4)(Ar)$ and $V^+(CH_4)_n$ (n=2-4) complexes can be found in a previous paper by our group.[53] Briefly, the methane molecules bind to vanadium in an η^2 orientation for $V^+CH_4(Ar)$ and $V^+(CH_4)_4$. For $V^+(CH_4)_2$, the lowest energy geometry was found to be between η^2 and η^3 with an angle of 156°. For $V^+(CH_4)_3$, one methane is η^2 and the other two are nearly η^2.

B. $V_2^+(CH_4)_n$ (n=1-4)

Vanadium dimer and its cation are well characterized experimentally, and theory and experiment are in good accord. Most experimental studies use resonant two-color photoionization (R2PI), as the resulting observation of V_2^+ ensures that the signal is due to V_2, rather than a larger cluster. Langridge-Smith *et al.*[54] used R2PI to measure the rotationally-resolved electronic spectrum near 700 nm and determined that the ground state of the neutral dimer is $^3\Sigma_g^-$, with a bond length of 1.77 Å.[54] From the short bond length they concluded that the *3d* electrons contribute significantly to the bonding. At higher energies of the first photon, the R2PI signal abruptly drops, as predissociation becomes so rapid that it outcom-

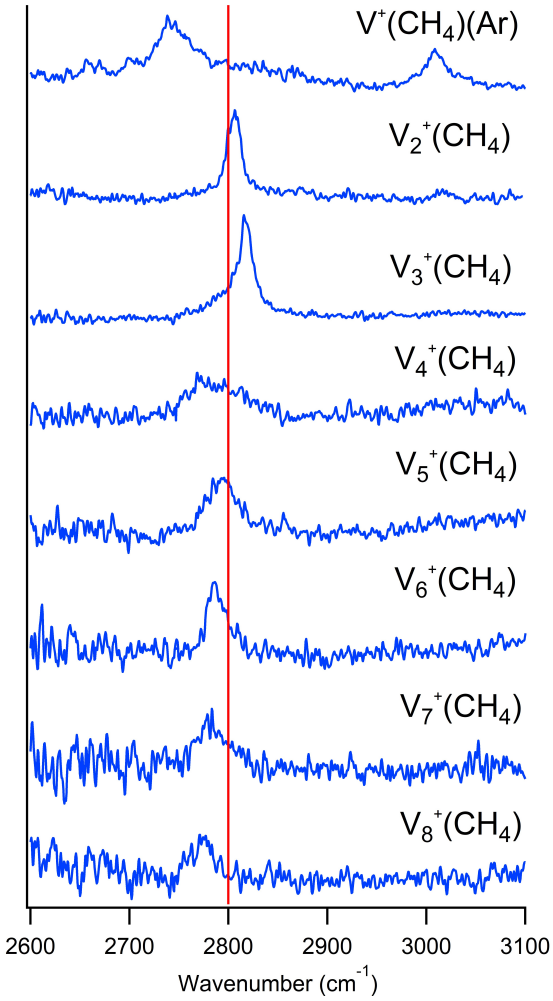

FIG. 1. Experimental photodissociation spectra of $V_x^+(CH_4)$ (x=1-8) in the C−H stretching region. The y-axis shows the normalized photofragment yield. A line at 2800 cm^{-1} is drawn to facilitate comparison of peak positions.

petes ionization by the second photon. This allowed Spain *et al.*[55] to determine the BDE of V_2 as 2.753±0.001 eV. Subsequently, James *et al.*[56] also used R2PI, varying the energy of the second photon, to determine the ionization energy of V_2 as 6.3565±0.0006 eV.

There have been several DFT calculations on V_2. Zhang *et al.*[57] have reviewed previous studies and evaluated the performance of 43 density functionals for BDE(V_2). They conclude that the errors in the calculated BDEs (which are substantial) are primarily due to errors in the calculated energy gap between the *4s* and *3d* atomic orbitals of the vanadium atom. Hübner and Himmel[58] measured the electronic spectrum of V_2 in a Ne matrix and also carried out extensive MRCI+Q calculations of low-lying singlet, triplet, and quintet states.

TABLE I. Calculated binding energies of $V_2^+(CH_4)_n$ (n=1-4), $V_3^+(CH_4)_n$ (n=1-3), $V_4^+(CH_4)_n$ (n=1-2), and $V_x^+(CH_4)$ (x=5-8)[a]

Species	S[b]	cm^{-1}	kJ/mol
$V_2^+-CH_4$[c]	2	5127	61
$V_2^+CH_4-CH_4$[c]	2	4795	57
$V_2^+(CH_4)_2-CH_4$[c]	2	2287	27
$V_2^+(CH_4)_3-CH_4$[c]	2	2594	31
$V_3^+-CH_4$	5	3071	37
$V_3^+CH_4-CH_4$	5	2242	27
$V_3^+(CH_4)_2-CH_4$	5	2182	26
$V_4^+-CH_4$	2	3407	41
$V_4^+(CH_4)-CH_4$	2	2691	32
$V_5^+-CH_4$	5	2736	33
$V_6^+-CH_4$	2	3627	43
$V_7^+-CH_4$	1	3400	41
$V_8^+-CH_4$[d]	2	2112	25

[a]Calculations are at zero Kelvin at the B3LYP+D3/6-311++G(3df,3pd) level of theory [b]Spin multiplicity [c]The BDEs are to the spin allowed doublet (S=2); they are 201 cm^{-1} lower to the quartet (S=4) ground state. [d]The quartet (S=4) is 820 cm^{-1} above the ground state (S=2) and its BDE to V_8^+ (S=4) is 5522 cm^{-1}.

They predict a $^3\Sigma_g^-$ ground state with r=1.804 Å, in good agreement with experiment. The next lowest energy states ($^1\Sigma_g^+$ and $^1\Gamma_g$) are calculated to be only 440 and 580 cm^{-1} above the ground state. The lowest quintet state ($^5\Delta_u$) is much higher in energy, at 7820 cm^{-1}.

The cation is also well-characterized experimentally. The R2PI study of James *et al.*[56] determined that its ground state is $^4\Sigma_g^-$. Su *et al.*[30] used collision-induced dissociation (CID) to determine BDE(V_2^+)=3.13±0.14 eV. Russon *et al.*[59] observed a photodissociation onset at 3.140±0.002 eV and assigned this as BDE(V_2^+). This assignment is confirmed by the internal consistency of a thermodynamic cycle with BDE(V_2),[55] IE(V_2)[56] and IE(V). Yang *et al.*[60] used PFI-ZEKE spectroscopy to determine the bond length of V_2^+ (r=1.7347(24)

Å). The cation has a slightly shorter and stronger bond than the neutral.

An early DFT calculation by Simard *et al.*[61] predicts a $^4\Sigma_g^-$ ground state with r=1.741 Å, in excellent accord with experiment. DFT calculations also often predict a low-lying doublet state ($^2\Delta_g$), for example at 2300 cm^{-1} using the PW86-P86 functional.[62] As part of a study of reactions of V_2^+ with CO_2, Li *et al.*[63] carried out calculations on V_2^+ at several levels of theory. They note the challenges in using DFT and, in their highest-level calculation (ZORA-NEVPT2), predict a $^4\Sigma_g^-$ ground state with the $^2\Delta_g$ state only 250 cm^{-1} higher in energy. Our calculations at the MRCI+Q/aug-cc-pVQZ level predict a $^4\Sigma_g^-$ ground state with r=1.760 Å. The $^2\Delta_g$ state is predicted to be only 1811 cm^{-1} higher in energy and to have r=1.790 Å. Our B3LYP+D3/6-311++G(3df,3pd) calculations find that the ground state for V_2^+ is a quartet, with r=1.698 Å. The doublet is only 201 cm^{-1} higher in energy and has a shorter V−V bond length (r=1.628 Å).

In our previous work on complexes of metal cations and metal cluster ions with methane, we found that the B3LYP functional successfully reproduces the measured experimental spectra. This is despite the well-documented deficiencies in this functional's treatment of metal clusters.[64,65] However, functionals that better model metal-metal interactions, such as BPW91, often do not do as well as B3LYP in reproducing how interaction with the metal affects covalent bonds in an organic ligand, which is what these experiments are sensitive to.[38,39] As a result, in this study we calculated structures and spectra using both B3LYP+D3 and BPW91+D2. The later functional has been extensively used to model metal cluster ions, including V_x^+.[48,66–69] As shown in Table S2, BPW91+D2 better reproduces experimental sequential V_x^+-V bond strengths than does B3LYP+D3. However, BPW91 is slightly worse at reproducing the vibrational spectra of $V_x^+(CH_4)$ and is substantially worse for $V_x^+(CH_4)_n$ (n>1). As a result, simulations using B3LYP+D3 are shown here and those using BPW91+D2 are in the SI.

Once a methane molecule is added to V_2^+, the doublet becomes the ground state. For $V_2^+(CH_4)$, the doublet is 1662 cm^{-1} more stable than the quartet; this gap increases to 4111 cm^{-1} in $V_2^+(CH_4)_2$ and remains similar for $V_2^+(CH_4)_3$ and $V_2^+(CH_4)_4$ (4018 and 4053 cm^{-1}, respectively). The primary difference between quartet and doublet V_2^+ is that the quartet has an electron in a σ^* molecular orbital that is a combination of d_{z^2} (where z is the V-V axis) and s with substantial electron density on the z axis, away from the V-V bond. As a result of repulsion between methane and the electron in this orbital, CH_4 binds to quartet

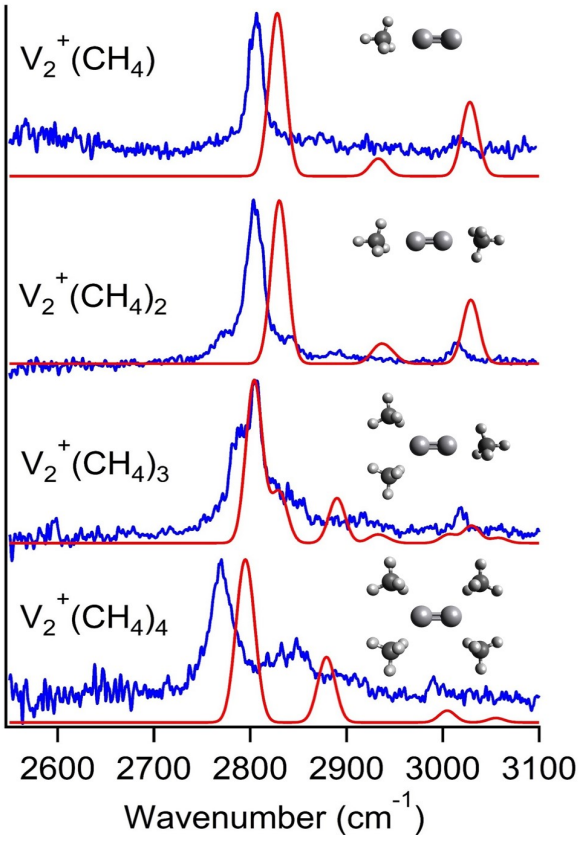

FIG. 2. Experimental photodissociation spectra (blue) and simulated (red) spectra of doublet $V_2^+(CH_4)_n$ (n=1-4) in the C−H stretching region. The calculations are done at the B3LYP+D3 level of theory with the 6-311++G(3dp,3df) basis set.

V_2^+ with a VVC angle of 134°. In contrast, for the doublet, the VVC atoms are collinear, so there is stronger interaction between the CH_4 and V for the first two methanes, which bind on the z axis.

The experimental spectra of $V_2^+(CH_4)_n$ (n=1-4), Figure 2, show a peak near 2800 cm^{-1} for n=1-2. For n=3, a shoulder appears at 2780 cm^{-1} and the major peak shifts down to 2760 cm^{-1} for n=4. This suggests a different methane binding coordination as more methane molecules are added. The experimental spectra also contain a small peak around 3000 cm^{-1}.

The spectra of $V_2^+(CH_4)$ and $V_2^+(CH_4)_2$ have an intense peak at 2806 and 2803 cm^{-1}, respectively, and a weak peak at 3015 cm^{-1}. The binding energies of the first and second methane are calculated to be 5127 and 4795 cm^{-1} (Table I) which means that observed dissociation is likely due to IRMPD. The red shift increases as more methanes are added, which is a bit surprising, but appears to be mostly due to going from η^3 to η^2 coordination.

The calculations qualitatively reproduce the change in red shift.

The calculation for $V_2^+(CH_4)$ predicts the V-V-C-H atoms are nearly collinear and the methane has η^3 hydrogen coordination ($\angle$H−C−V=180°; r_{V-C}= 2.404 Å). The simulation predicts a peak at 2828 cm^{-1} and a peak at 3028 cm^{-1} with half the intensity. In both cases, the lower energy peak corresponds to the proximate C−H symmetric stretch and the higher energy peak to the free distal C−H stretch of an η^3 methane. These are 22 and 13 cm^{-1} higher, respectively, than is observed.

For $V_2^+(CH_4)_2$, the calculation predicts two η^3 methane molecules ($\angle$H−C−V= 177, 179°; r_{V-C}= 2.414 and 2.411 Å) offset from each other by 60°. It is slightly distorted from D_{3d} symmetry. The simulation predicts an intense peak at 2830 cm^{-1} and a less intense peak at 3029 cm^{-1}. As with $V_2^+(CH_4)$, the calculated frequencies are slightly higher than is observed. The spectrum also has a shoulder to the red of the main peak. This is likely due to a small population of ions with both methanes bound to the same vanadium atom. This leads to coordination closer to η^2 and a more red-shifted absorption, as discussed below.

The experimental spectrum of $V_2^+(CH_4)_3$ has an intense peak at 2805 cm^{-1} with a shoulder around 2839 cm^{-1} and weak peaks at 2915 and 3019 cm^{-1}. In $V_2^+(CH_4)_4$, the intense peak is at 2770 cm^{-1} with a less intense peak at 2833 and weak peaks at 2889 and 2990 cm^{-1}. The binding energy of the third methane is 2287 cm^{-1}, significantly less than the first two, and the fourth methane is 2594 cm^{-1}, slightly higher than third methane.

The $V_2^+(CH_4)_3$ calculation predicts an η^3 methane ($\angle$H−C−V=178°; r_{V-C}= 2.418 Å) on one vanadium atom and two almost η^2 methanes ($\angle$H−C−V=140°; r_{V-C}= 2.565 Å) on the other. The simulation predicts a peak at 2804 cm^{-1} with a shoulder around 2829 cm^{-1} and two smaller peaks at 2890 and 3029 cm^{-1}. The first peak (2804 cm^{-1}) corresponds to the proximate symmetric stretches of the two η^2 methanes and the shoulder is the proximate symmetric stretch of the η^3 methane. The two smaller peaks correspond to the proximate antisymmetric stretch of the η^2 methanes (2890 cm^{-1}) and the free distal stretch of the η^3 methane (3029 cm^{-1}). The simulated spectrum is an excellent match to experiment.

The $V_2^+(CH_4)_4$ calculation predicts a square planar orientation with all four methanes nearly equivalent. They all have almost η^2 orientation with $\angle$H−C−V=2@141° and 2@142° (r_{V-C}= 2@2.525, 2@2.539 Å). The simulation predicts an intense peak at 2795 cm^{-1} due to the proximate symmetric C−H stretch vibrations, a weaker peak at 2879 cm^{-1} from the corresponding antisymmetric stretches, and a weak peak at 3004 cm^{-1} due to the distal

symmetric C−H stretch. The BPW91+D2 calculated spectra are very similar to those of B3LYP+D3 for $V_2^+(CH_4)_n$ (n=1,2) (Figure S3). For n=3,4 it predicts that the lowest C-H stretch is too red shifted. This was also the case for $Fe_2^+(CH_4)_3$.[38]

To summarize, the first two methanes bind in an η^3 orientation and have only one intense peak due to the symmetric stretch. Each vanadium atom has one or no methanes bound to it. To accommodate a third methane, the binding orientation of the two methane on one vanadium atom changes to almost η^2, while the methane on the other vanadium atom remains η^3. The main peak is now the symmetric proximate C-H stretch of the η^2 methanes, while the η^3 peak has shifted to slightly higher wavenumber. For $V_2^+(CH_4)_4$ all four methanes have nearly η^2 orientation. As a result, the intense peak shifts to lower wavenumber. A second peak, due to the corresponding antisymmetric stretches in the η^2 methanes, appears at n=3 and becomes more intense for n=4. The n=1-3 complexes also have a weak peak around 3019 cm^{-1}; for n=4, this peak is red shifted by 20 cm^{-1}.

C. $V_3^+(CH_4)_n$ (n=1-3)

Although experiment and theory are in agreement on the geometries and low-lying electronic states of $V_2^{0,+}$ there is a great deal of debate over the ground states and geometries (equilateral or isosceles) of $V_3^{0,+}$. Cox *et al.*[70] determined IE(V_3)=5.49±0.05 eV by measuring its photoionization efficiency. Yang *et al.*[71] refined this to 5.4978 ± 0.0004 eV and observed vibrational structure using PFI-ZEKE. Calaminici *et al.*[62] used the PW86-P86 functional with a GGA optimized basis set to calculate low-lying electronic states of V_3 and V_3^+ and predict the ZEKE spectrum. They predict that V_3 is equilateral (D_{3h} symmetry), with a $^2A_1'$ ground state with r_{V-V}=2.169 Å. Only 0.03 eV higher in energy is a $^4A_2$ state with an acute structure (C_{2v} symmetry) with r_{V-V}=2@2.335 Å; 1.964 Å. For the cation, they predict an equilateral $^3A_2'$ ground state with r_{V-V}=2.180 Å, and an equilateral $^1A_1'$ state at 0.18 eV. Their calculated ZEKE spectrum is in good agreement with experiment. Subsequently, Ford and Mackenzie[72] used mass-analyzed threshold ionization (MATI) to obtain higher resolution and extend the spectrum to higher energies. Their spectrum is generally consistent with this calculation, and they assign most of the spectrum as being due to the $^3A_2' \leftarrow {}^2A_1'$ transition. They determine that the cation $^1A_1'$ excited state is very low-lying, only 14 cm^{-1} above the ground state. Cation vibrational frequencies (for the

$^3A_2'$ state) are determined to be ω_1 (E')=200±1 cm^{-1} and ω_3 (A_1)=442±1 cm^{-1}. By fitting partially-resolved rotational structure, they determine r=2.217±0.001 Å. Ratsch *et al.*[32] measured the far-IR vibrational spectra of V_x^+ (x=3-15) using argon tagging at the FELIX free-electron laser facility. They observe a peak at 231 cm^{-1} for V_3^+(Ar). The discrepancy with the MATI result is too large to be due to perturbation of the vibration by the argon, but it's possible that argon stabilizes the singlet more than the triplet, making it the ground state, and ω_1 is calculated to be 13 cm^{-1} higher in the $^1A_1'$ state than in the $^3A_2'$ state.[62] DFT calculations carried out in support of the vibrational spectra[32] predict only isosceles structures. The ground state is a singlet, but its calculated spectrum is a poor match to experiment. The best match is with a triplet structure at 0.11 eV with r_{V-V}=2@2.24 Å; 2.04 Å. There have been several other DFT calculations of V_3^+; they generally predict a triplet ground state, but the geometry ranges from equilateral[66] to isosceles with one short and two long V-V bonds,[48,73–75] depending on the functional and basis set.

In the current study, the B3LYP+D3 calculations find that V_3^+ has a quintet ground state with V−V bond lengths of 2@2.540 and 2.977 Å with an apex angle of 72°. The triplet is 1935 cm^{-1} higher in energy and has V−V bond lengths of 1.692, 2.706, and 2.721 Å. Geometry optimizations begun with C_{2v} symmetry for the triplet revert to this asymmetric structure. The geometry of the triplet is similar to that found in many previous DFT calculations, but the results differ from most of those obtained using other functionals in predicting a quintet ground state. Its geometry is unusual in that the bonds are all fairly long and the apex angle is >60°. In our study, multiple calculations were run from geometries identified in previous studies, but they relaxed to the isosceles structure shown here, or a similar one higher in energy. Our calculations also predict that the quintet remains the ground state for $V_3^+(CH_4)_n$ (n=1-3).

Inspired by the multi-reference configuration interaction (MRCI) calculations on Nb_3 and Nb_3^+ by Addicoat and Metha,[76,77] we carried out MCSCF and MRCI calculations on V_3 and V_3^+. However, calculations on the vanadium clusters were far more challenging, as the bonds are much weaker. The V_2^+-V bond strength is only 219 kJ/mol,[30] compared to 490 kJ/mol for Nb_2^+-Nb.[78] Details of the calculations are given in the SI (Section S2). Only equilateral and C_{2v} geometries were considered. At the MRCI+Q/cc-pVTZ level, V_3 is predicted to have a $^4A_2$ ground state, with one short bond (r=1.85 Å) and two long bonds (3.27 Å). V_3^+ is calculated to have a $^5A_2$ ground state, again with an acute structure (one bond at 1.94 Å

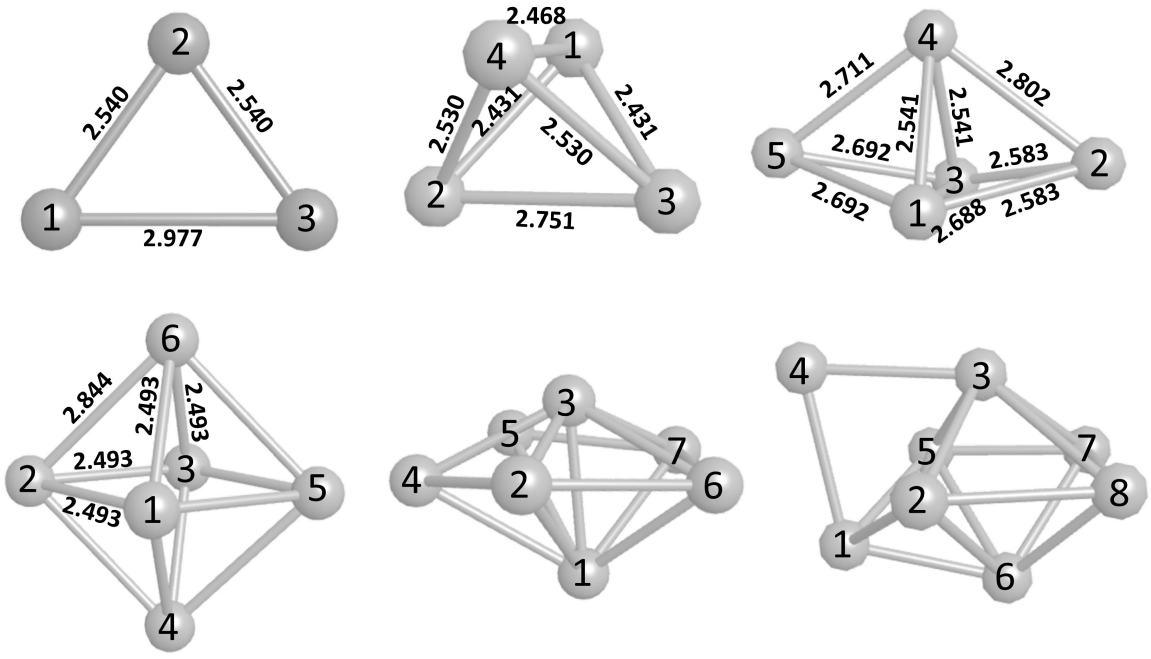

FIG. 3. Geometries of the lowest energy structures of the V_x^+ (x=3-8) clusters with the atoms numbered. Bond lengths are in Å. Calculations were done at the B3LYP+D3/6-311++G(3df,3pd) level of theory.

and two at 2.94 Å). The lowest triplet state ($^3B_1$) has a similar structure (2.05 Å, 2@2.90 Å) and is 4020 cm^{-1} higher in energy. Septet states are higher still. Equilateral structures were investigated, but were found to be significantly higher in energy and to have rather long bonds: for the quintet, r=2.72 Å (at 7113 cm^{-1}) and for the triplet, r=2.77 Å (3167 cm^{-1} above $^3B_1$).

The experimental spectra of $V_3^+(CH_4)_n$ (n=1-3) (Figure 4) all show a peak near 2815 cm^{-1}. There is an additional peak near 2790 cm^{-1} for $V_3^+(CH_4)_2$; this becomes the most intense peak in the $V_3^+(CH_4)_3$ spectrum. To keep track of which vanadium atom(s) is binding to methane, Figure 3 shows the calculated geometries of $V_{3\text{-}8}^+$ with the atoms numbered and the bond lengths for $V_{3\text{-}6}^+$. For V_3^+ the V1 and V3 atoms are equivalent. The corresponding figure for BPW91+D2 is in the SI (Figure S4).

The experimental spectrum of $V_3^+(CH_4)$ has an intense, sharp peak at 2816 cm^{-1}. The calculation predicts the methane binds to V1 with coordination between η^2 and η^3 ($\angle$H−C−V=156°; r_{V-C}= 2.482 Å). The calculated methane binding energy is 3071 cm^{-1}.

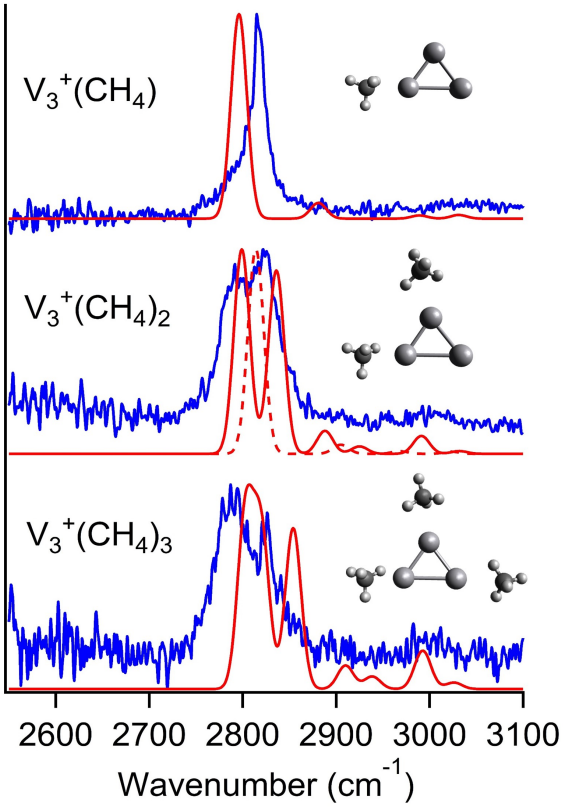

FIG. 4. Experimental photodissociation spectra (blue) and simulated spectra (red) of quintet $V_3^+(CH_4)_n$ (n=1-3) in the C−H stretching region. The calculations are done at the B3LYP+D3/6-311++G(3dp,3df) level of theory and show their corresponding geometries. The red dotted simulation for $V_3^+(CH_4)_2$ corresponds to a structure with two equivalent CH_4.

The simulation predicts a peak at 2796 cm^{-1}, 20 cm^{-1} more red shifted than experiment. This peak is the proximate symmetric C−H stretch.

The experimental spectrum of $V_3^+(CH_4)_2$ has two intense peaks at 2788 and 2819 cm^{-1}. The calculations predict two nearly iso-energetic isomers. The lowest energy isomer has two equivalent methanes (bound to V1 and V3 with ∠H−C−V=165°; r_{V-C}= 2.495 Å). The calculated binding energy is 2242 cm^{-1}. The calculated spectrum consists of a single peak at 2814 cm^{-1} shown in Figure 4. The second isomer is only 25 cm^{-1} higher in energy. One methane binds to V1 with ∠H−C−V=156° (r_{V-C}= 2.502 Å) and the other one to V2 with ∠H−C−V=157° (r_{V-C}= 2.656 Å). The simulated spectrum of this isomer (Figure 4) consists of two intense peaks, which correspond to the proximate symmetric C−H stretch of the closer methane (2799 cm^{-1}) and then the farther methane (2836 cm^{-1}). This asymmetrical isomer

is a much better match to experiment.

The experimental spectrum of $V_3^+(CH_4)_3$ has an intense, wide peak at 2787 cm^{-1} and a weaker, sharper peak at 2826 cm^{-1}. The calculations predict that each methane binds to a different vanadium and the binding energy of the third methane is 2182 cm^{-1}. The calculation predicts the methane molecules are between η^2 and η^3 ($\angle$H−C−V= 157, 157, 161°; r_{V-C}= 2.551, 2.678, 2.721 Å) on V1, V3, and V2, respectively. The simulation predicts a peak at 2803 cm^{-1} with a shoulder at 2820 cm^{-1} and a peak at 2854 cm^{-1}. The peaks correspond to the proximate symmetric C−H stretches of the methane with the shorter V-C bond length (larger red shift) to the longer V-C bond length (smaller red shift).

In summary, the calculations predict that binding to the equivalent vanadium atoms V1 and V3 leads to a larger red shift than binding to V2. They also predict that the first CH_4 binds to V1, next to V2, then to V3. The experimental spectra show that the first CH_4 gives the smallest red shift and is due to binding to the unique vanadium atom (V2); additional CH_4 bind to V1 and V3 and give larger red shifts.

The vibrational spectra of $V_3^+(CH_4)_n$ (n=2,3) show that the methane molecules in these complexes are not equivalent. This is replicated in our DFT calculations. We thus conclude that, in the these complexes, the vanadium atoms are not equivalent and the V_3^+ core is not equilateral. This differs from the results of Ford *et al.*[72], who observed rotational structure in the MATI spectrum and assigned it to an equilateral structure of V_3^+ with r_{V-V}= 2.217±0.001 Å. One possible way to reconcile these findings is that binding methane changes the geometry and/or spin state of the complex.

At the BPW91+D2 level, V_3^+ is isosceles, so one vanadium should offer a very different binding environment than the other two. However, when methane binds, the same C-H stretching spectrum is predicted, irrespective of the binding site. As a result, in the predicted spectra (Figure S6) for $V_3^+(CH_4)_n$ (n=1-3) each has only one peak, in clear disagreement with experiment.

D. $V_4^+(CH_4)$

There have been several experimental and numerous computational studies of V_4 and V_4^+. Yang *et al.*[79] used PFI-ZEKE photoelectron spectroscopy to measure the ionization energy of V_4 (5.6591±0.0004 eV) with greater accuracy than previously done by Cox *et al.*

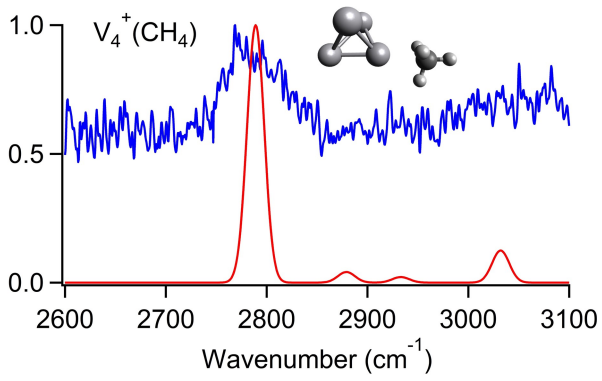

FIG. 5. Experimental photodissociation spectrum (blue), simulated spectrum (red), and the optimized geometry of doublet $V_4^+(CH_4)$ at the B3LYP+D3/6-311++G(3df,3pd) level of theory.

(5.63±0.05 eV).[70] The far-IR vibrational spectrum[32] of V_4^+ consists of a strong peak at 198 cm^{-1} and a weak peak at 255 cm^{-1}. Minemoto *et al.*[80] measured the electronic spectrum of V_4^+ from 440 to 1750 nm by monitoring loss of argon from $V_4(Ar)^+$. The spectrum is broad, with a peak at 1100 nm and a more intense peak at 500 nm.

Computational studies of V_4 and V_4^+ predict a planar or tetrahedral ground state, depending on the level of theory. A study using tight binding theory by Zhao *et al.*[81] finds the neutral V_4 cluster to adopt a tetrahedral geometry while a gradient-corrected local spin density DFT study by Grönbeck and Rosén[73] predicts the same cluster to have a planar geometry, with the tetrahedron 0.33 eV higher in energy. They also predict IE(V_4)=5.5 eV, in good agreement with experiment.

A later DFT study of V_4 and V_4^+ using the BPW91 functional by Wu and Ray[66] finds the tetrahedron to be the lowest energy isomer in both cases, and predicts IE=5.105 eV, about 0.5 eV below experiment. DFT calculations by Minemoto *et al.*[80] in support of their experimental study also find V_4^+ to be a distorted tetrahedron with C_{2v} symmetry. Local spin density approximation calculations by Li *et al.*[74] report a planar structure for V_4^+ with the tetrahedron 0.12 eV higher in energy. DFT (PBE) calculations by Ratsch *et al.*[32] find the V_4^+ geometry is a trigonal pyramid and that the planar structure is much higher in energy (0.79 eV). The calculated vibrational frequencies for the lowest energy structure match their measured far-IR spectrum, while those of the planar isomer are too low. A recent DFT with dispersion (BPW91+D2) study by Meza *et al.*[48] report that V_4^+ forms a planar trapezoid structure. However, their calculated vibrational frequencies do not match the experimental

spectrum of Ratsch *et al.*[32] BP86+D3 calculations by Zhang *et al.*[75] also predict that V_4^+ is planar.

In this study, at the B3LYP+D3/6-311++G(3df,3pd) level of theory, we find that V_4^+ is a doublet and adopts a distorted tetrahedral geometry. As shown in Figure 3, V1 and V4 are equivalent, as are V2 and V3. The quartet is 3959 cm^{-1} higher in energy and has a similar structure to the doublet.

The experimental spectrum of $V_4^+(CH_4)$ (Figure 5) has a broad peak around 2780 cm^{-1} on top of continuous dissociation. We have observed broad, non-resonant dissociation in other systems[53] and attribute it to electronic transition(s) to low-lying excited states. The calculation predicts that the methane binds to V1 with nearly η^3 coordination ($\angle$H−C−V= 172°; r_{V-C}= 2.382 Å) and a binding energy of 3407 cm^{-1}. The calculated vibrational spectrum is dominated by a peak at 2789 cm^{-1} which corresponds to the proximate symmetric C−H stretch. Since the geometry of $V_4^+(CH_4)$ is nearly tetrahedral, the binding sites are nearly equivalent and the predicted spectra of the $V_4^+(CH_4)$ isomers are the same.

The experimental spectrum of $V_4^+(CH_4)_2$ (Figure S8) has a peak at 2770 cm^{-1}. The binding energy of the second methane is 2691 cm^{-1}. The calculation predicts two equivalent methanes with $\angle$H−C−V= 155° and r_{V-C}= 2.487 Å on V1 and V4. The single peak in the simulated spectrum at 2793 cm^{-1} corresponds to the proximate symmetric C−H stretch.

Several studies previously mentioned found a planar structure for V_4^+. We investigated planar structures and found a local minimum geometry that is nearly, but not quite, planar, with two vanadium atoms out of plane with the other two in a boat-like geometry. However, according to our calculations this isomer is 5743 cm^{-1} higher in energy and is not likely to form. In addition, when methane binds to it, the C−H stretch is predicted to be 2732 cm^{-1}, which is too red shifted to match the experimental spectrum. At the BPW91+D2 level, V_4^+ is planar (rhombus). The predicted spectra at the two distinct binding sites (Figure S9) are slightly more red shifted than is observed. The major peak in the experimental spectrum of $V_4^+(CH_4)$ is significantly broader than those of the other $V_x^+(CH_4)$, suggesting contributions from multiple metal cluster isomers and/or distinct methane binding sites. This is not consistent with the only metal isomer present being (quasi-) tetrahedral. So, it is likely that the metal core is planar, although a tetrahedral structure may also contribute.

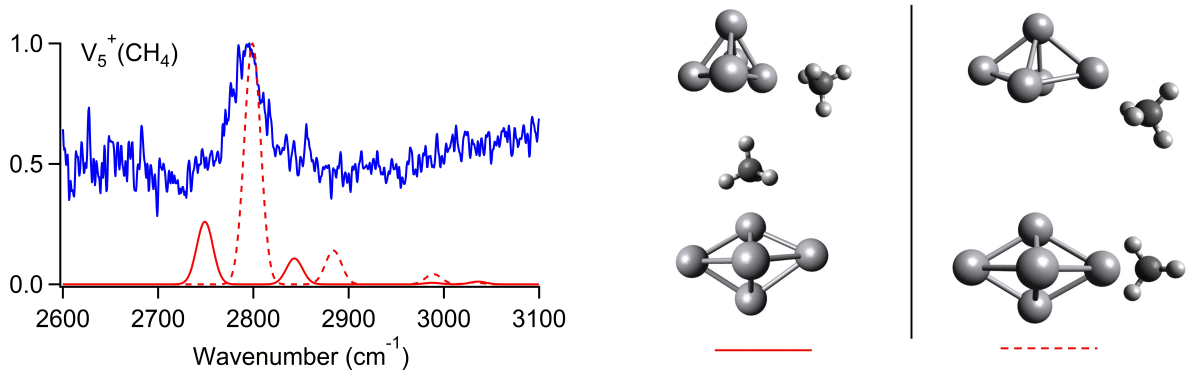

FIG. 6. Experimental photodissociation spectrum (blue), simulated spectra (red), and the optimized geometry of quintet $V_5^+(CH_4)$ shown from two different angles at the B3LYP+D3/6-311++G(3df,3pd) level of theory. On the left is the lowest energy isomer (red line) in which the methane binds to an equatorial vanadium (V1) and the right shows the next lowest energy isomer (red dashed line) in which the methane binds to an axial vanadium (V5). The relative intensities of the simulated spectra reflect the calculated absorption intensities.

E. $V_5^+(CH_4)$

Theory on neutral V_5 has been done by several groups. Most studies predict a trigonal bipyramidal geometry,[48,73,74,82] although others find a heavily distorted square pyramid geometry.[66,75] In calculations to support their far-infrared spectra of V_5^+, Ratsch *et al.*[32] find a slightly distorted square pyramid geometry. However, a trigonal bipyramid structure is close in energy and provides the best match to their experimental spectrum. Meza *et al.*[48] also predict a distorted trigonal bipyramid.

In this study, V_5^+ is a quintet and has a distorted trigonal bipyramidal geometry with C_s symmetry (Figure 3). The singlet is 1259 cm^{-1} higher in energy and the triplet is 2753 cm^{-1} above the quintet. Simulations were run with methane binding to V1, V2, V4, and V5. V3 is equivalent to V1. The two lowest-energy isomers are discussed here.

The experimental spectrum of $V_5^+(CH_4)$, Figure 6, has a peak at 2793 cm^{-1} on top of constant dissociation. In the lowest energy isomer, the methane binds to an equatorial vanadium atom (V1) with coordination between η^2 and η^3 (H−C−V= 151°; r_{V-C}= 2.432 Å). The binding energy is 3141 cm^{-1}. The simulation predicts two relatively weak peaks at 2749 and 2843 cm^{-1}. The peaks correspond to the symmetric and antisymmetric C-H

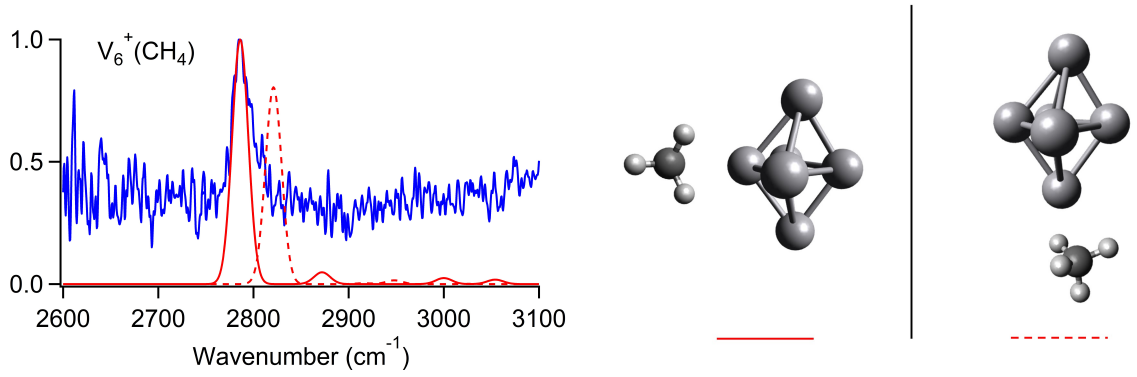

FIG. 7. Experimental photodissociation spectrum (blue), simulated spectra (red), and the optimized geometry of doublet $V_6^+(CH_4)$ at the B3LYP+D3/6-311++G(3df,3pd) level of theory. The lowest energy isomer, in which the methane binds to an equatorial vanadium (V3), is shown on the left and the next lowest energy isomer, in which methane binds to an axial vanadium (V5), is on the right.

stretch. This simulation (Figure 6) is a poor match to the experiment as it predicts a doublet and neither peak matches the peak in the experiment.

There is another isomer 405 cm^{-1} higher in energy (Table I), in which the methane binds to an axial vanadium atom (V5). The methane coordination is similar, between η^2 and η^3 (H−C−V= 155°), but the V-C bond length is significantly longer, r_{V-C}= 2.502 Å. This simulation predicts an intense peak at 2799 cm^{-1}, 6 cm^{-1} red shifted from the experimental peak. The peak corresponds to the symmetric C-H stretch in CH_4. The axial isomer is the best match to experiment. At the BPW91+D2 level, the spectra of the two isomers are more similar (Figure S10), so the axial isomer is likely but not definitively the isomer observed.

F. $V_6^+(CH_4)$

Ratsch *et al.*[32] calculated a tetragonal bipyramid (distorted octahedron) geometry for V_6^+, which agrees with previous theoretical results.[66,73,82,83] Their calculations found several isomers with different aspect ratios, all close in energy and with similar infrared spectra, all of which are in good agreement with their experiment. A distorted trigonal prism is significantly higher in energy (although it was identified as the ground state in another study[48]) and does not match experiment.

Our calculations predict that the bare V_6^+ cluster (Figure 3) is a quartet and forms a slightly distorted octahedron (r_{V-V}= 8@2.493, 4@2.844 Å). The doublet is 590 cm^{-1} higher in energy and forms a more distorted octahedron. When a methane molecule is added, the doublet becomes the ground state, only 197 cm^{-1} below the quartet. The core V_6^+ structure distorts more when the methane is added, where V4 and V6 become slightly closer together and move closer to V3 and farther from V1.

The experimental spectrum of $V_6^+(CH_4)$, Figure 7, has a peak at 2786 cm^{-1} on top of a constant dissociation background, likely due to absorption to low-lying electronic state(s). The calculation predicts the methane binds to V3 in an almost η^2 coordination (H−C−V= 144°; r_{V-C}= 2.487 Å) with a binding energy of 3627 cm^{-1}. The second lowest energy isomer predicts the methane binds to V5 with nearly η^3 coordination (H−C−V= 174°; r_{V-C}= 2.455 Å) and a binding energy of 3299 cm^{-1} (Table I).

The simulation of the lowest energy isomer predicts an intense peak at 2786 cm^{-1}, which matches exactly with experiment, and corresponds to the proximate symmetric C-H stretch. The simulation of the second lowest energy isomer predicts an intense peak at 2821 cm^{-1}, which is 35 cm^{-1} blue shifted from the experimental peak. The quartet state is calculated to lie at 197 cm^{-1} and to have a peak at 2814 cm^{-1}. In this case, the lowest energy isomer is the best match to experiment, and the spectrum is consistent with a distorted octahedral V_6^+ core in its doublet spin state. At the BPW91+D2 level, the core geometry is a distorted trigonal prism and the calculated spectrum (Figure S11) is slightly too red shifted.

G. $V_7^+(CH_4)$

Ratsch *et al.*[32] predict several low-lying isomers for V_7^+, all of which adopt distorted pentagonal bipyramid geometries. This is in agreement with other theoretical results.[48,66,73–75] However, the resulting simulated IR spectra are not a great match to their experimental spectrum.

Our calculation agrees with those of Ratsch: the bare V_7^+ cluster (shown in Figure 3) is a singlet and forms a distorted pentagonal bipyramid structure. V3 is closer to the pentagon than V1 and V4 is out of the plane of the other atoms in the pentagon. The triplet and quintet are 4371 and 1430 cm^{-1} higher in energy, respectively.

The experimental spectrum of $V_7^+(CH_4)$, Figure 8, has a peak at 2783 cm^{-1} on top of

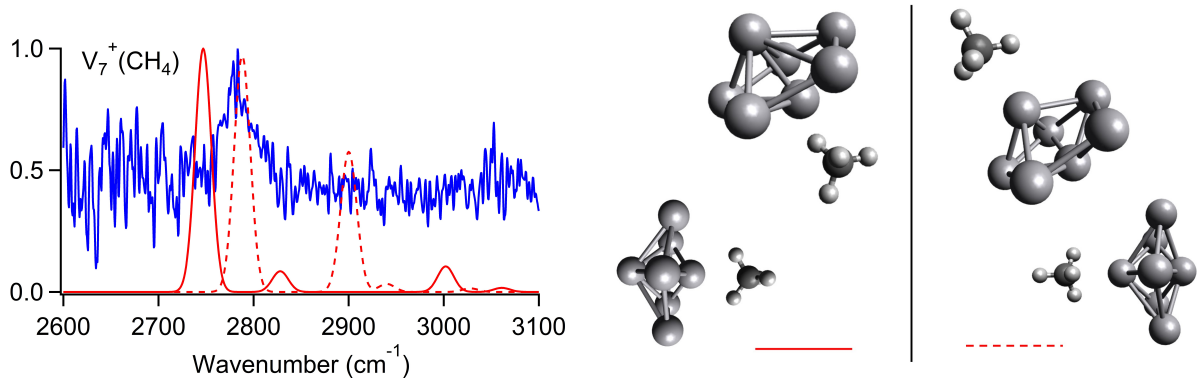

FIG. 8. Experimental photodissociation spectrum (blue), simulated spectra (red), and optimized geometries of singlet $V_7^+(CH_4)$ shown from two different angles at the B3LYP+D3/6-311++G(3df,3pd) level of theory. The lowest energy isomer is shown on the left and the second lowest energy isomer is on the right.

constant dissociation. In the lowest energy isomer, the methane binds to V3 with a binding energy of 3400 cm^{-1} in an almost η^2 orientation (H−C−V= 131°; r_{V-C}= 2.506 Å). The simulation predicts a weak peak at 2747 cm^{-1}. There is another isomer 201 cm^{-1} higher in energy in which methane binds to V1 in an almost η^3 orientation (H−C−V= 171°; r_{V-C}= 2.416 Å). This simulation predicts a weak peak at 2788 cm^{-1} and an even less intense peak at 2900 cm^{-1}.

Calculations in which methane binds to the equatorial vanadium atoms predict additional low-lying isomers. V2 and V5 to V7 are almost equivalent, so there are only two different binding sites on the equatorial vanadium atoms, V2 and V4. V4 is the vanadium atom that is out of plane with the others in the pentagon. Isomers with methane binding to V2 and V4 are 903 and 1195 cm^{-1} above the lowest energy isomer, respectively (Figure S14). Methane binds to the V2 and V4 vanadium atoms with coordination between η^3 and η^2, (H−C−V= 152°; r_{V-C}= 2.560 Å) and (H−C−V= 160°; r_{V-C}= 2.543 Å), respectively. The simulations predict a peak at 2808 cm^{-1} for V2 and at 2814 cm^{-1} for V4 with nearly the same intensities (which are twice as intense as the lowest energy isomers). All predicted peaks are due to the symmetric C-H stretch. It is difficult to assign a best match with these results and nothing can be said definitively. The lowest energy isomer (V3) predicts a peak that is more red shifted than experiment. The second lowest energy isomer (V1) matches the experimental peak almost perfectly, but predicts a second peak at 2900 cm^{-1}

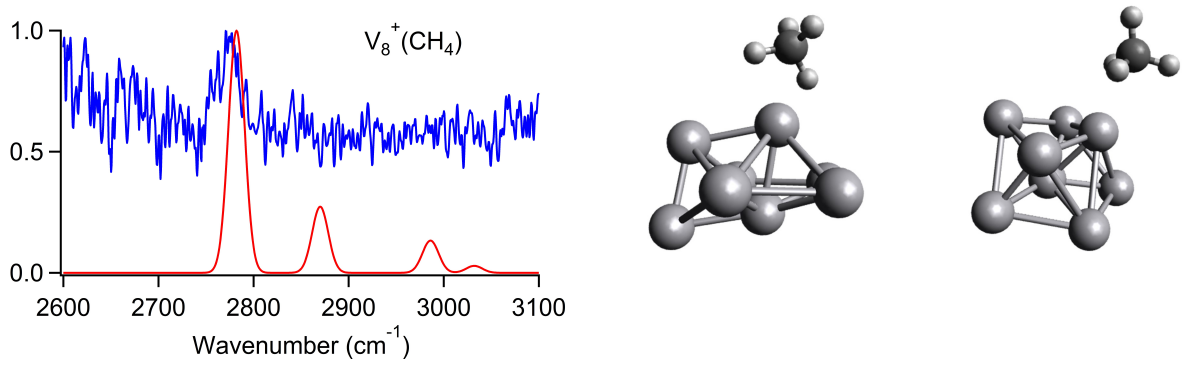

FIG. 9. Experimental photodissociation spectrum (blue), simulated spectrum (red), and the optimized geometry of doublet $V_8^+(CH_4)$ shown from two different angles at the B3LYP+D3/6-311++G(3df,3pd) level of theory.

that is not observed. The equatorial isomers (V2, V4) are higher in energy and would each lead to a single, intense peak that is less red shifted than experiment. The BPW91+D2 calculations predict that axial binding leads to a larger red shift than equatorial (Figure S12), with equatorial providing a better match to experiment.

H. $V_8^+(CH_4)$

For V_8^+, Ratsch *et al.*[32] predict a bicapped tetragonal bipyramid (bicapped octahedron) in the doublet spin state which agrees with other theoretical results.[48,66,73–75] The calculated spectrum is a good match to the experimental IR spectrum,[31,32] which has many peaks.

Our calculations also predict that the bare V_8^+ cluster is a doublet and forms a distorted bicapped octahedron, as shown in Figure 3. A hexagonal bipyramid is slightly higher in energy. The quartet, also a bicapped octahedron, is 1924 cm^{-1} above the ground state. Addition of methane reduces this gap, with quartet $V_8^+(CH_4)$ 820 cm^{-1} above the doublet ground state. Methane binding distorts the doublet more than the quartet.

The experimental spectrum of $V_8^+(CH_4)$, Figure 9, has a peak at 2771 cm^{-1} on top of constant dissociation. The lowest energy isomer is a doublet; the methane binds to V6 with coordination between η^2 and η^3 (H−C−V= 153°; r_{V-C}= 2.545 Å) and a binding energy of 2112 cm^{-1}.

Calculations were run with the methane bound to V1, V3, V4, and V6. Of these, V1 and

V6 have the lowest energy. The simulations of the doublet and quartet V1 and V6 isomers are plotted in Figure S15. The simulations for this molecule all predict a peak around the same place: 2753-2786 cm^{-1}. This makes it impossible to determine the structure observed. Based solely on relative energies, it would be the doublet V6 isomer. The BPW91+D2 and B3LYP+D3 calculations predict very similar structures and spectra (Figure S13).

I. Effect of charge

Although the average charge per atom decreases with increasing cluster size, x, these clusters are not symmetrical, so the charge is not equally distributed. We examined the calculated Mulliken charge on each metal atom to investigate whether methane preferentially binds to vanadium atoms with higher local charge and to what extent the methane perturbs the charges on the metal atoms. The results are summarized in Table S3. For x=3-5, all the atoms have similar charges and the CH_4 doesn't always bind to the one with the highest charge. For x=6-8, most of the charge is localized on just a few atoms. The CH_4 binds to an atom with higher than average charge, but not necessarily to the one with the highest charge. When CH_4 binds to a metal atom, the charge on that atom is almost always reduced (except for x=7). The V_x^+-CH_4 bond dissociation energies are similar for x=3-8, so it does not depend on the average charge per atom, and is not strongly affected by the charge on the atom that the methane binds to, so there likely is a significant covalent component to the BDEs.

IV. SUMMARY AND CONCLUSIONS

Methane binds intact to vanadium cluster ions, and the resulting $V_x^+(CH_4)_n$ (x=2-8) have red shifts of 102 to 146 cm^{-1} in the lowest-frequency C-H stretch. Clusters with x=2 and 3 have the smallest red shifts, while those with x=4-8 have significantly larger shifts. In $V_2^+(CH_4)_n$ (n=1-4), there is a larger red shift as more methanes are added due to the methane orientation changing from η^3 to η^2. The spectra of $V_3^+(CH_4)_n$ n=2,3 have two peaks, indicating that the methanes are not equivalent, which also implies that the vanadium atoms are not equivalent. The calculations predict an isosceles structure for the metal cluster and that there is a larger red shift when methane binds to either of the equivalent vanadium

atoms. The methane binds in an η^3 orientation, with different V-C bond lengths, the shorter of which leads to a larger red shift.

The spectrum of $V_4^+(CH_4)$ is significantly broader than those of the other clusters, indicating that multiple isomers contribute to the spectrum. This may include ones with planar and tetrahedral V_4^+ cores. The geometry of V_5^+ is a distorted trigonal bipyramid, with methane likely binding to an axial vanadium. The methane coordination is between η^2 and η^3. The geometry of V_6^+ is a slightly distorted octahedron, with the methane binding in an η^2 coordination. The calculation predicts that there is a spin change from quartet to doublet when methane is added, and the calculated spectrum for the doublet state matches experiment.

For $V_7^+(CH_4)$, the calculations predict a distorted pentagonal bipyramid core. There are several low energy isomers with very similar simulated spectra, all of which are in good agreement with experiment, so we cannot assign a binding site. For V_8^+, the calculations predict the structure is a distorted bicapped octahedron. As with $V_7^+(CH_4)$, there are several low energy isomers whose simulated spectra are a good match to experiment.

If the metal-methane interaction were purely electrostatic, then we would expect that the red shifts would decrease as cluster size increases because the charge on each metal atom is reduced. So, the observation that $V_x^+(CH_4)$ clusters with x=4-8 have significantly larger shifts than smaller clusters implies increased covalency in the metal-methane interaction for the larger clusters. However, this analysis also needs to consider the hydrogen coordination, as η^2 typically gives larger red shifts than η^3, and the smaller clusters are η^3, while the larger ones are mostly closer to η^2. Despite this, there remains a larger red shift for the larger clusters even when coordination is considered. Both $V_2^+(CH_4)$ and $V_7^+(CH_4)$ (second lowest isomer) have η^3 coordination and the calculations predict a 40 cm^{-1} larger red shift for the larger cluster. So, even taking the change in coordination into account, the larger clusters show more covalency.

Although odd clusters are more reactive than even ones with D_2,[28] there is no even/odd trend in the red shifts with methane. Instead, our results suggest that V_5^+ to V_8^+ would be more reactive with methane than V_2^+ and V_3^+, and there would be little difference in reactivity of even and odd clusters.

In addition, these results show that vibrational spectra of the C-H stretches in methane attached to metal clusters can, in some cases, reveal the geometry and spin state of the

metal cluster, with the caveat that the methane may in some cases perturb the structure of the metal cluster. This is helpful, as more direct experimental methods of characterizing the structure and spin states of metal clusters are very challenging. The vibrational spectra are at low frequencies and have low intensity, and calculated spectra of different isomers are often similar, while photoionization spectra become very congested and difficult to interpret for clusters larger than trimers and those with a large geometry change upon ionization. Transition metal clusters are challenging to calculate, have many low-lying electronic states, and often do not have much symmetry.

Supporting Information The Supporting Information is available free of charge at (url inserted by journal).
Full references 45 and 52; details on experimental methods (Section S1) and MRCI calculations (Section S2); flow reactor source (Figure S1); B3LYP and BPW91 BDE table (Table S1); sequential vanadium binding energies B3LYP and BPW91 (Table S2); vibrational spectra of $V_2^+(CH_4)_n$ (n=1-4) with B3LYP (Figure S2) and with BPW91 (Figure S3); Mulliken charges (Table S3); $V_{3\text{-}8}^+$ geometries using BPW91 (Figure S4); vibrational spectra of $V_3^+(CH_4)_n$ (n=1-3) with B3LYP (Figure S5) and with BPW91 (Figure S6); geometry of V_3^+ (Figure S7); vibrational spectrum of $V_4^+(CH_4)_2$ with B3LYP (Figure S8) and with BPW91 (Figure S9); vibrational spectrum of $V_5^+(CH_4)$ with BPW91 (Figure S10); vibrational spectrum of $V_6^+(CH_4)$ with BPW91 (Figure S11); vibrational spectrum of $V_7^+(CH_4)$ with BPW91 (Figure S12); vibrational spectrum of $V_7^+(CH_4)$ and simulated spectra of two isomers (Figure S14); vibrational spectrum of $V_8^+(CH_4)$ with BPW91 (Figure S13); vibrational spectrum of $V_8^+(CH_4)$ and simulated spectra of four isomers (Figure S15); energies, vibrational frequencies, intensities and geometries of each complex at the B3LYP+D3/6-311++G(3df,3pd) level of theory (Tables S4 to S10).

ACKNOWLEDGMENTS

Financial support from the National Science Foundation under award no. CHE-1856490 is gratefully acknowledged. The authors are grateful for computational resources provided by the Massachusetts Green High-Performance Computing Center (MGHPCC). We thank Dr. Miguel Castro for providing details on the BPW91+D2 calculations.

Data Availability Statement

The data that support the findings of this study are available from the corresponding author upon reasonable request.

REFERENCES

[1]M. C. Alvarez-Galvan, N. Mota, M. Ojeda, S. Rojas, R. Navarro, and J. L. G. Fierro, "Direct Methane Conversion Routes to Chemicals and Fuels," Catal. Today **171**, 15–23 (2011).

[2]H. Jahangiri, J. Bennett, P. Mahjoubi, K. Wilson, and S. Gu, "A Review of Advanced Catalyst Development for Fischer-Tropsch Synthesis of Hydrocarbons from Biomass Derived Syn-gas," Catal. Sci. Technol. **4**, 2210–2229 (2014).

[3]D. H. R. Barton, "The Invention of Chemical Reactions," Aldrichim. Acta **23**, 3–10 (1990).

[4]K. K. Irikura, J. L. Beauchamp, and A. Amos, "Electronic Structure Considerations for Methane Activation by Third-Row Transition-Metal Ions," J. Phys. Chem **95**, 8344–8351 (1991).

[5]A. Shayesteh, V. V. Lavrov, G. K. Koyanagi, and D. K. Bohme, "Reactions of Atomic Cations with Methane: Gas Phase Room-Temperature Kinetics and Periodicities in Reactivity," J. Phys. Chem. A **113**, 5602–5611 (2009).

[6]J. Roithová and D. Schröder, "Selective Activation of Alkanes by Gas-Phase Metal Ions," Chem. Rev. **110**, 1170–1211 (2010).

[7]J. Roithová and J. M. Bakker, "Ion Spectroscopy in Methane Activation," Mass Spectrom. Rev. **41**, 513–528 (2022).

[8]S. M. Lang, A. Frank, and T. M. Bernhardt, "Activation and Catalytic Dehydrogenation of Methane on Small Pd_x^+ and Pd_xO^+ Clusters," J. Phys. Chem. C **117**, 9791–9800 (2013).

[9]G. Kummerlöwe, I. Balteanu, Z. Sun, O. P. Balaj, V. E. Bondybey, and M. K. Beyer, "Activation of Methane and Methane-d_4 by Ionic Platinum Clusters," Int. J. Mass Spectrom. **254**, 183–188 (2006).

[10]M. Schlangen and H. Schwarz, "Effects of Ligands, Cluster Size, and Charge State in Gas-Phase Catalysis: A Happy Marriage of Experimental and Computational Studies," Catal. Lett. **142**, 1265–1278 (2012).

[11]A. Fielicke, "Probing the Binding and Activation of Small Molecules by Gas-Phase Tran-

sition Metal Clusters via IR Spectroscopy," Chem. Soc. Rev. **52**, 3778–3841 (2023).

[12]D. Schröder, S. Shaik, and H. Schwarz, "Two-state Reactivity as a New Concept in Organometallic Chemistry," Acc. Chem. Res. **33**, 139–145 (2000).

[13]P. Armentrout, "Reactions and Thermochemistry of Small Transition Metal Cluster Ions," Annu. Rev. Phys. Chem. **52**, 423–461 (2001).

[14]S. M. Lang and T. M. Bernhardt, "Gas Phase Metal Cluster Model Systems for Heterogeneous Catalysis," Phys. Chem. Chem. Phys. **14**, 9255–9269 (2012).

[15]H. Schwarz, "How and Why Do Cluster Size, Charge State, and Ligands Affect the Course of Metal-Mediated Gas-Phase Activation of Methane?" Isr. J. Chem. **54**, 1413–1431 (2014).

[16]Z. Luo, A. W. Castleman, and S. N. Khanna, "Reactivity of Metal Clusters," Chem. Rev. **116**, 14456–14492 (2016).

[17]P. B. Armentrout, "Gas-Phase Perspective on the Thermodynamics and Kinetics of Heterogeneous Catalysis," Catal. Sci. Technol. **4**, 2741–2755 (2014).

[18]Y. X. Zhao, Z. Y. Li, Y. Yang, and S. G. He, "Methane Activation by Gas Phase Atomic Clusters," Acc. Chem. Res. **51**, 2603–2610 (2018).

[19]B. Yuan, S. Y. Tang, and S. Zhou, "Size Effects in Gas-phase C-H Activation," Chem. Phys. Chem. **24**, e202200769 (2022).

[20]Y. Yang, Y. X. Zhao, and S. G. He, "Conversion of CH_4 Catalyzed by Gas Phase Ions Containing Metals," Chem. Eur. J. **28**, e202200062 (2022).

[21]R. Liyanage, X.-G. Zhang, and P. B. Armentrout, "Activation of Methane by Size-Selected Iron Cluster Cations, Fe_n^+ (n=2-15): Cluster-CH_x (x=0-3) Bond Energies and Reaction Mechanisms," J. Chem. Phys. **115**, 9747–9763 (2001).

[22]F. Liu, X. G. Zhang, R. Liyanage, and P. B. Armentrout, "Methane Activation by Nickel Cluster Cations, Ni_n^+ (n=2-16): Reaction Mechanisms and Thermochemistry of Cluster-CH_x (x=0-3) Complexes," J. Chem. Phys. **121**, 10976–10990 (2004).

[23]A. Nakajima, T. Kishi, Y. Sone, S. Nonose, and K. Kaya, "Reactivity of Positively Charged Cobalt Cluster Ions with CH_4, N_2, H_2, C_2H_4, and C_2H_2," J. Phys. D Atoms, Molecules and Clusters **19**, 385–387 (1991).

[24]Y.-M. Chen and P. B. Armentrout, "Activation of Methane by Gas-Phase Rh^+," J. Phys. Chem. **99**, 10775–10779 (1995).

[25]G. Albert, C. Berg, M. Beyer, U. Achatz, S. Joos, G. Niedner-Schatteburg, and V. E. Bondybey, "Methane Activation by Rhodium Cluster Argon Complexes," Chem. Phys.

Lett. **268**, 235–241 (1997).

[26]J. F. Eckhard, T. Masubuchi, M. Tschurl, R. N. Barnett, U. Landman, and U. Heiz, "Room-Temperature Methane Activation Mediated by Free Tantalum Cluster Cations: Size-by-size Reactivity," J. Phys. Chem. A **125**, 5289–5302 (2021).

[27]U. Achatz, C. Berg, S. Joos, B. S. Fox, M. K. Beyer, G. Niedner-Schatteburg, and V. E. Bondybey, "Methane Activation by Platinum Cluster Ions in the Gas Phase: Effects of Cluster Charge on the Pt_4 Tetramer," Chem. Phys. Lett. **320**, 53–58 (2000).

[28]M. R. Zakin, D. M. Cox, R. O. Brickman, and A. Kaldor, "Benzene C-D Bond Activation by Free Vanadium Cluster Cations," J. Phys. Chem. **93**, 6823–6827 (1989).

[29]R. Liyanage, J. Conceição, and P. B. Armentrout, "Guided Ion Beam Studies of the Reactions of V_n^+ (n=2-13) with D_2: Cluster-Deuteride Bond Energies as a Chemical Probe of Cluster Electronic Structure," J. Chem. Phys. **116**, 936–945 (2002).

[30]C.-X. Su, D. A. Hales, and P. B. Armentrout, "Collision-Induced Dissociation of V_n^+ (n=2-20) with Xe: Bond Energies, Dissociation Pathways, and Structures," J. Chem. Phys. **99**, 6613–6623 (1993).

[31]A. Fielicke, A. Kirilyuk, C. Ratsch, J. Behler, M. Scheffler, G. von Helden, and G. Meijer, "Structure Determination of Isolated Metal Clusters via Far-Infrared Spectroscopy," Phys. Rev. Lett. **93**, 023401 (2004).

[32]C. Ratsch, A. Fielicke, A. Kirilyuk, J. Behler, G. von Helden, G. Meijer, and M. Scheffler, "Structure Determination of Small Vanadium Clusters by Density-Functional Theory in Comparison with Experimental Far-Infrared Spectra," J. Chem. Phys. **122**, 124302 (2005).

[33]A. S. Chaves, M. J. Piotrowski, and J. L. F. Da Silva, "Evolution of the Structural, Energetic, and Electronic Properties of the 3d, 4d, and 5d Transition-Metal Clusters (30 TM_n systems for n = 2-15): A Density Functional Theory Investigation," Phys. Chem. Chem. Phys. **19**, 15484–15502 (2017).

[34]A. Fielicke, P. Gruene, G. Meijer, and D. M. Rayner, "The Adsorption of CO on Transition Metal Clusters: A Case Study of Cluster Surface Chemistry," Surf. Sci. **603**, 1427–1433 (2009).

[35]S. Dillinger, J. Mohrbach, and G. Niedner-Schatteburg, "Probing Cluster Surface Morphology by Cryo Spectroscopy of N_2 on Cationic Nickel Clusters," J. Chem. Phys. **147**, 184305 (2017).

[36]A. Straßner, C. Wiehn, M. P. Klein, D. V. Fries, S. Dillinger, J. Mohrbach, M. H. Prosenc,

P. B. Armentrout, and G. Niedner-Schatteburg, "Cryo Spectroscopy of N_2 on Cationic Iron Clusters," J. Chem. Phys. **155**, 244305 (2021).

[37]M. Citir, G. Altinay, G. Austein-Miller, and R. B. Metz, "Vibrational Spectroscopy and Theory of $Fe^+(CH_4)_n$ (n=1-4)," J. Phys. Chem. A **114**, 11322–11329 (2010).

[38]M. A. Ashraf, C. W. Copeland, A. Kocak, A. R. McEnroe, and R. B. Metz, "Vibrational Spectroscopy and Theory of $Fe_2{}^+(CH_4)_n$ (n=1-3)," Phys. Chem. Chem. Phys. **17**, 25700–25704 (2015).

[39]C. W. Copeland, M. A. Ashraf, E. M. Boyle, and R. B. Metz, "Vibrational Spectroscopy of $Fe_3{}^+(CH_4)_n$ (n=1-3) and $Fe_4{}^+(CH_4)_4$," J. Phys. Chem. A **121**, 2132–2137 (2017).

[40]O. V. Lushchikova, S. Reijmer, P. B. Armentrout, and J. M. Bakker, "IR Spectroscopic Characterization of Methane Adsorption on Copper Clusters $Cu_n{}^+$(n=2-4)," J. Am. Soc. Mass Spectrom. **33**, 1393–1400 (2022).

[41]D. J. Harding, C. Kerpal, G. Meijer, and A. Fielicke, "Activated Methane on Small Cationic Platinum Clusters," Angew. Chem., Int. Ed. Engl. **51**, 817–819 (2012).

[42]I. Swart, A. Fielicke, B. Redlich, G. Meijer, B. M. Weckhuysen, and F. M. De Groot, "Hydrogen-Induced Transition from Dissociative to Molecular Chemisorption of CO on Vanadium Clusters," J. Am. Chem. Soc. **129**, 2516–2520 (2007).

[43]T. Jaeger, A. Fielicke, G. von Helden, G. Meijer, and M. Duncan, "Infrared Spectroscopy of Water Adsorption on Vanadium Cluster Cations ($V_x{}^+$; x=3-18)," Chem. Phys. Lett. **392**, 409–414 (2004).

[44]J. Husband, F. Aguirre, P. Ferguson, and R. B. Metz, "Vibrationally Resolved Photofragment Spectroscopy of FeO^+," J. Chem.. Phys. **111**, 1433–1437 (1999).

[45]M. J. Frisch, G. W. Trucks, H. B. Schlegel, G. E. Scuseria, M. A. Robb, J. R. Cheeseman, G. Scalmani, V. Barone, B. Mennucci, G. A. Petersson, *et al.*, "Gaussian 09 Revision D.01," (2013), Gaussian Inc. Wallingford CT.

[46]K. Raghavachari, "Perspective on "Density Functional Thermochemistry. III. The Role of Exact Exchange"," Theor. Chem. Acc. **103**, 361–363 (2000).

[47]S. Grimme, J. Antony, S. Ehrlich, and H. Krieg, "A Consistent and Accurate ab initio Parametrization of Density Functional Dispersion Correction (DFT-D) for the 94 Elements H-Pu," J. Chem. Phys. **132** (2010).

[48]B. Meza, P. Miranda, and M. Castro, "Structural and Electronic Properties of Hydrated V_nH_2O and $V_n{}^+H_2O$, n≤13, Systems," J. Phys. Chem. C **121**, 4635–4649 (2017).

[49]S. Grimme, "Semiempirical GGA-type Density Functional Constructed with a Long-Range Dispersion Correction," J. Comput. Chem. **27**, 1787–1799 (2006).

[50]J. Wang, J. Han, X. Xie, Z. Xue, C. Fliedel, and R. Poli, "$FeBr_2$-Catalyzed Bulk ATRP Promoted by Simple Inorganic Salts," Macromol. **52**, 5366–5376 (2019).

[51]H. J. Werner, P. J. Knowles, G. Knizia, F. R. Manby, and M. Schütz, "Molpro: A General-Purpose Quantum Chemistry Program Package," WIREs Computat. Mol. Sci. **2**, 242–253 (2012).

[52]H. J. Werner, P. J. Knowles, G. Knizia, F. R. Manby, M. Schütz, P. Celani, W. Györffy, D. Kats, T. Korona, R. Lindh, *et al.*, "MOLPRO, ver. 2015.1, A Package of ab initio Programs," University of Cardiff Chemistry Consultants (UC3): Cardiff, Wales, UK (2015).

[53]J. Kozubal, T. Heck, and R. B. Metz, "Structures of $M^+(CH_4)_n$ (M=Ti,V) Based on Vibrational Spectroscopy and Density Functional Theory," J Phys Chem A **125**, 4143–4151 (2021).

[54]P. R. Langridge-Smith, M. D. Morse, G. P. Hansen, R. E. Smalley, and A. J. Merer, "The Bond Length and Electronic Structure of V_2," J. Chem. Phys. **80**, 593–600 (1984).

[55]E. M. Spain and M. D. Morse, "Bond Strengths of Transition-Metal Dimers: TiV, V_2, TiCo, and VN," J. Phys. Chem. **96**, 2479–2486 (1992).

[56]A. M. James, P. Kowalczyk, E. Langlois, M. D. Campbell, A. Ogawa, and B. Simard, "Resonant Two Photon Ionization Spectroscopy of the Molecules V_2, VNb, and Nb_2," J. Chem. Phys. **101**, 4485–4495 (1994).

[57]W. Zhang, D. G. Truhlar, and M. Tang, "Explanation of the Source of Very Large Errors in Many Exchange-Correlation Functionals for Vanadium Dimer," J. Chem. Theory Comput. **10**, 2399–2409 (2014).

[58]O. Hübner and H. J. Himmel, "Low-Energy Excited States of Divanadium: A Matrix Isolation and MRCI Study," Phys. Chem. Chem. Phys. **18**, 14667–14677 (2016).

[59]L. M. Russon, S. A. Heidecke, M. K. Birke, J. Conceicao, M. D. Morse, and P. B. Armentrout, "Photodissociation Measurements of Bond Dissociation Energies: Ti_2^+, V_2^+, Co_2^+, and Co_3^+," J. Chem. Phys. **100**, 4747–4755 (1994).

[60]D. S. Yang, A. M. James, D. M. Rayner, and P. A. Hackett, "Pulsed Field Ionization Zero Kinetic Energy Photoelectron Spectroscopy of the Vanadium Dimer Molecule," J. Chem. Phys. **102**, 3129–3134 (1995).

[61]B. Simard, A. M. James, P. Kowalczyk, R. Fournier, and P. A. Hackett, "High-Resolution

Spectroscopy of Small Transition Metal Molecules: Recent Experimental and Theoretical Progress on Group 5 Diatomics," in *Laser Techniques for State-Selected and State-to-State Chemistry II*, Vol. 2124, edited by J. W. Hepburn, International Society for Optics and Photonics (SPIE, 1994) pp. 376 – 387.

[62]P. Calaminici, A. M. Köster, T. Carrington, P. N. Roy, N. Russo, and D. R. Salahub, "V_3: Structure and Vibrations from Density Functional Theory, Franck-Condon Factors, and the Pulsed-Field Ionization Zero-Electron-Kinetic Energy Spectrum," J. Chem. Phys. **114**, 4036–4044 (2001).

[63]J. Li, C. Geng, T. Weiske, and H. Schwarz, "Counter-Intuitive Gas-Phase Reactivities of $[V_2]^+$ and $[V_2O]^+$ towards CO_2 Reduction: Insight from Electronic Structure Calculations," Ang. Chem. Int. Ed. **59**, 12308–12314 (2020).

[64]N. E. Schultz, Y. Zhao, and D. G. Truhlar, "Databases for Transition Element Bonding: Metal-Metal Bond Energies and Bond Lengths and their Use to Test Hybrid, Hybrid Meta, and Meta Density Functionals and Generalized Gradient Approximations," J. Phys. Chem. A **109**, 4388–4403 (2005).

[65]J. Paier, M. Marsman, and G. Kresse, "Why Does the B3LYP Hybrid Functional Fail for Metals?" J. Chem. Phys. **127**, 024103 (2007).

[66]X. Wu and A. K. Ray, "A Density Functional Study of Small Neutral and Cationic Vanadium Clusters V_n and V_n^+ (n=2-9)," J Chem. Phys. **110**, 2437–2445 (1999).

[67]G. L. Gutsev, M. D. Mochena, and C. W. Bauschlicher, "Structure and Properties of Mn_n, Mn_n^-, and Mn_n^+ Clusters (n = 3-10)," J. Phys. Chem. A **110**, 9758–9766 (2006).

[68]G. L. Gutsev, C. A. Weatherford, P. Jena, E. Johnson, and B. R. Ramachandran, "Structure and Properties of Fe_n, Fe_n^-, and Fe_n^+ Clusters, n=7-20," J. Phys. Chem. A **116**, 10218–10228 (2012).

[69]M. Ichihashi, T. Hanmura, and H. Odaka, "Dissociative Adsorption of N_2 onto Size-Selected Ti_n^+ and Ti_nO^+ ($n \leq 16$) Toward Nitrogen Fixation," J. Phys. Chem. A **125**, 5048–5053 (2021).

[70]D. Cox, R. Whetten, M. Zakin, D. Trevor, K. Reichmann, and A. Kaldor, *AIP Conference Proceedings 146, Optical Science and Engineering Ser. 6, Advances in Laser Science, Vol. 1*, edited by M. L. W.C. Stwalley (AIP, New York, 1986) p. 527.

[71]D. S. Yang, A. M. James, D. M. Rayner, and P. A. Hackett, "Pulsed Field Ionization Zero Kinetic Energy Photoelectron Spectroscopy of Small Vanadium Clusters. Using Velocity

Slip as a Mass Selector," Chem. Phys. Lett. **231**, 177–182 (1994).

[72]M. S. Ford and S. R. MacKenzie, "Preparing Transition-Metal Clusters in Known Structural Forms: The Mass-Analyzed Threshold Ionization Spectrum of V_3," J. Chem. Phys. **123**, 84308 (2005).

[73]H. Grönbeck and A. Rosén, "Geometric and Electronic Properties of Small Vanadium Clusters: A Density Functional Study," J. Chem. Phys. **107**, 10620–10625 (1997).

[74]S. Li, M. M. G. Alemany, and J. R. Chelikowsky, "Ab initio Calculations for the Photoelectron Spectra of Vanadium Clusters," J. Chem. Phys. **121**, 5893–5898 (2004).

[75]H. Zhang, H. Wu, Y. Jia, B. Yin, L. Geng, Z. Luo, and K. Hansen, "Hydrogen Release From a Single Water Molecule on V_n^+ ($3 \leq n \leq 30$)," Commun. Chem **3**, 1–10 (2020).

[76]M. A. Addicoat and G. F. Metha, "Excited States of Nb_3N_2 and Nb_3C_2: Density Functional Theory, CASSCF, and MRCI Studies," J. Chem. Phys. **130**, 164308 (2009).

[77]M. Addicoat, *Computational Investigations into the Structure and Reactivity of Small Transition Metal Clusters*, Ph.D. thesis, University of Adelaide (2009).

[78]D. A. Hales, L. Lian, and P. B. Armentrout, "Collision-Induced Dissociation of Nb_n^+ (n=2-11): Bond Energies and Dissociation Pathways," Int. J. Mass Spectrom. **102**, 269–301 (1990).

[79]D. S. Yang and P. A. Hackett, "ZEKE Spectroscopy of Free Transition Metal Clusters," J. Electron Spectrosc. **106**, 153–169 (2000).

[80]S. Minemoto, A. Terasaki, H. Imoto, and T. Kondow, "Electronic Structure of Vanadium Tetramer Ion Studied by Optical Absorption Spectroscopy," J. Chem. Phys. **109**, 9737–9743 (1998).

[81]J. Zhao, X. Chen, Q. Sun, F. Liu, G. Wang, and K. D. Lain, "Tight-Binding Study of the Structural and Magnetic Properties of Vanadium Clusters," Phys. B: Condens. Matter **215**, 377–382 (1995).

[82]H. Sun, Y.-H. Luo, J. Zhao, G. Wang, and Y. Cheng, "Structural, Electronic, and Magnetic Properties of Small Vanadium Clusters," Phys. Stat. Sol. (B) **215**, 1127–1135 (1999).

[83]A. Taneda, T. Shimizu, and Y. Kawazoe, "Stable Disordered Structures of Vanadium Clusters," J. Condens Matter. Phys. **13**, L305 (2001).